Journal of Archaeological Science 133 (2021) 105442

Contents lists available at ScienceDirect

Journal of Archaeological Science

journal homepage: www.elsevier.com/locate/jas

Modeling avian eggshell microstructure to predict ontogenetic age and reveal patterns of human-avifauna interaction

Kristina Douglass [a,b,c,*], Priyangi Bulathsinhala [d], Teresa J. Feo [c,e], Tim Tighe [f], Scott Whittaker [g], Zanell Brand [h], Helen James [c], Torben Rick [b]

[a] Department of Anthropology and Institutes of Energy and the Environment, The Pennsylvania State University, University Park, PA, USA
[b] Department of Anthropology, National Museum of Natural History, Smithsonian Institution, Washington, DC, USA
[c] Department of Vertebrate Zoology, Division of Birds, National Museum of Natural History, Smithsonian Institution, Washington, DC, USA
[d] Department of Statistics, The Pennsylvania State University, University Park, PA, USA
[e] California Council on Science and Technology, Sacramento, CA, USA
[f] Materials Characterization Lab, The Pennsylvania State University, University Park, PA, USA
[g] Scanning Electron Microscopy Laboratory, National Museum of Natural History, Smithsonian Institution, Washington, DC, USA
[h] Oudtshoorn Research Farm, Elsenburg, Department of Agriculture, Western Cape Government, South Africa

ARTICLE INFO

Keywords:
Optical profilometry
Digital microscopy
Scanning electron microscopy
High-resolution computed tomography
Statistical modeling
Zooarchaeology
Birds
Ratites
Ostrich
Eggshell
Taphonomy

ABSTRACT

Archaeological eggshell is a commonly recorded, yet underutilized material for understanding human-environment interaction in the past. In addition to the use of archaeological eggshell as a paleoenvironmental proxy, archaeologists have innovated important new approaches to the study of archaeological avian eggshell, including the application of scanning electron microscopy (SEM) for the characterization of eggshell microstructures. These studies have demonstrated the importance of eggshell for understanding how ancient communities exploited and interacted with avifauna. In this paper, we build on these methodological advances by testing new approaches to image avian eggshell and characterizing complex eggshell surface microstructures. We demonstrate the utility of capturing high-resolution 3-dimensional (3D) eggshell surfaces using advanced imaging modalities (optical profilometry, scanning electron microscopy, digital microscopy, computed tomography), to model changes in eggshell microstructures that are correlated with ontogeny. Using the Common Ostrich (*Struthio camelus*) as our model system, we introduce a statistical modeling approach to predict the ontogenetic age of ratite eggshell using roughness measurements of 3D features. Successful prediction of ontogenetic age has great potential to reveal archaeological patterns of human exploitation of avian eggs. These findings further illustrate the importance of archaeological eggshell for investigating human-environment interactions, emphasizing the need for archaeologists to use field methods (hand/trowel excavation and fine mesh screen) that facilitate eggshell recovery.

1. Introduction

The archaeological record is replete with evidence of the importance of birds to human communities, extending to at least the Middle Stone Age in Africa when ostrich eggshell was engraved (Assefa et al., 2018; Texier et al., 2013; Texier et al., 2010) and the Upper Paleolithic in Europe when bird bones were transformed into some of the earliest known flutes (Conard et al., 2009). Birds are integral to human interaction, subsistence, ritual, migration and navigation, and the recovery and analysis of bird remains from archaeological sites yields crucial insights into the human past (Dirrigl et al., 2020; Serjeantson, 2009). Bird remains in archaeological sites include bones, gizzard stones, pellets, feathers, and eggshell. Despite the importance of birds to human societies and the abundance of bird remains in many archaeological sites around the world, several scholars have noted that avian eggshell remains an understudied component of the archaeological record (Beacham and Durand, 2007; Stewart et al., 2013a).

This paper describes approaches for high-resolution 3D imaging of avian eggshell and a statistical model for predicting eggshell ontogenetic age built using a time series of ostrich eggs (*Struthio camelus*). The aim of developing these methods is to increase archaeologists' ability to derive information about human-avifauna interactions from archaeological

* Corresponding author. Department of Anthropology and Institutes of Energy and the Environment, The Pennsylvania State University, University Park, PA, USA.
E-mail address: kdouglass@psu.edu (K. Douglass).

https://doi.org/10.1016/j.jas.2021.105442
Received 25 January 2021; Received in revised form 29 June 2021; Accepted 7 July 2021
Available online 29 July 2021

eggshell. Eggshell is a commonly recorded material in archaeological deposits and has been used successfully as a paleoenvironmental proxy and dating material through the analysis of eggshell geochemistry (Brooks et al., 1990; Donaire and López-Martínez, 2009; Ecker et al., 2015; Freundlich et al., 1989; Higham, 1994; Janz et al., 2009; Johnson et al., 1998; Clarke et al., 2007; Long et al., 1983; Vogel et al., 2001). Molecular techniques, including ancient DNA analysis (aDNA) and proteomics of archaeological avian eggshell elucidate bird population dynamics and taxonomy (Stewart et al., 2013a; Jacomb et al., 2014; Allentoft et al., 2014; Stewart et al., 2013b; Oskam et al., 2012; Oskam et al., 2010).

Relative to most other classes of archaeofaunal remains, however, morphological analysis of avian eggshell has rarely been used to understand human-avifauna interactions, including egg harvesting and husbandry practices. The first effort to encourage the morphological study of archaeological avian eggshell resulted in a manual for ootaxonomic identification, covering a range of avian families and species, based on Scanning Electron Microscopy (SEM) imagery (Sidell, 1993). Although ootaxonomic identification through morphological analysis of avian eggshell has proven challenging (Buss and Keiss, 2009), morphological analysis of anthropogenic modification of eggshell (esp. in the production of artifacts like eggshell beads and liquid containers) has enabled the study of human symbolic expression, craft production, interaction and exchange (Texier et al., 2013; Kandel and Conard, 2005; Wei et al., 2017; Jacobson, 1987). Others have distinguished anthropogenic modification in the production of liquid containers from similar patterns produced by carnivore predation (Kandel, 2004). Additional modifications on archaeological avian eggshell result from intentional and unintentional heat treatment (Miller et al., 2016; Taivalkoski and Holt, 2016).

Previous work to estimate the ontogenetic age of archaeological eggshell investigated potential husbandry of turkey (*Meleagris gallopavo*) in the ancient American Southwest and suggested that changes in eggshell microstructures were time-dependent and correlated with stages of embryonic growth (Beacham and Durand, 2007). During the course of incubation, developing avian embryos derive a substantial portion of the calcium they require for growth (>80%) by resorbing calcium carbonate from the surrounding eggshell (Carey, 1983). This process of resorption is enabled by the interaction between eggshell mammillary conesmicrostructures on the interior surface of avian eggshell (Fig. 1) — and the shell membranes (Burley and Vadehra, 1989). As a result of this process of resorption, the surface structure of eggshell mammillary cones changes over the course of incubation (Fig. 2). Furthermore, because resorption of eggshell calcium carbonate is linked to the development of the avian embryo (Blom and Lilja, 2004), changes in eggshell mammillary cone surface structure are hypothesized to be time-dependent, and thus indicative of the ontogenetic age of the embryo (Beacham and Durand, 2007).

Using two-dimensional (2D) SEM images of eggshell, Beacham and Durand qualitatively assessed changes in eggshell microstructures and demonstrated the possibility of identifying eggshell from hatched versus un-hatched turkey eggs in archaeological contexts (Beacham and Durand, 2007). Their work built upon previous documentation of the presence of turkey eggshell in Chaco Canyon deposits (Windes, 1987); they interpreted the high proportion of archaeological eggshell showing signs of significant resorption as evidence that ancient Chacoan communities were hatching turkey eggs, in order to raise chicks, as opposed to harvesting and consuming the egg contents (Beacham and Durand, 2007). Following this innovative approach, further studies were conducted on archaeological eggshell from the American Southwest (*M. gallopavo*), Oaxaca (*M. gallopavo*), and eastern Europe (*Gallus gallus*), further elucidating processes of avian domestication, the importance of bird husbandry, particularly during periods of climate downturn, and the ritual significance of fertilized eggs as grave goods (Conrad et al., 2016; Lapham et al., 2016; Jonuks et al., 2017).

Successful prediction of eggshell ontogenetic age has great potential to reveal archaeological patterns of human exploitation of avian taxa. As indicated by the studies referenced above, a primary question for archaeologists is whether we can use eggshell morphology to successfully distinguish between eggs from which a chick hatched naturally and eggs for which normal chick development was halted at some ontogenetic stage prior to hatching, potentially as a consequence of harvesting by people. Further questions regarding human behavior can also be posed, if our analytical methods allow us to identify more precisely the ontogenetic timing of egg harvesting. Evidence for the harvesting of fertilized eggs during later stages of embryogenesis, for example, may indicate dietary preferences (e.g. a preference for consuming a more developed chick embryo, as opposed to yolk and albumen).

In this paper, we develop a highly resolved ontogenetic time series of Common Ostrich (*Struthio camelus)* eggshell and a statistical model to predict the ontogenetic age of unknown eggshell samples. Although chicken is the classic model species in bird developmental biology, we selected ostrich as our model species to expand analytical possibilities with regard to ratites. Several ratite taxa have gone extinct over the course of the Holocene, including New Zealand's moa (Dinornithiformes) and Madagascar's elephant birds (Aepyornithidae). These extinctions often followed human dispersals to islands, and we know little regarding the potential contribution of ratite egg harvesting to the success of human communities in colonizing new environments, or to subsequent ratite population declines. Our work furthers the study of archaeological eggshell in three important ways:

1. We demonstrate the utility of capturing high-resolution three-dimensional (3D) eggshell surfaces using advanced imaging modalities (Optical Profilometry [OP], SEM, digital microscopy, Micro-Computed Tomography [micro-CT]), in order to **quantitatively model changes in eggshell microstructures that are correlated with ontogeny.** This allows us to compare different imaging

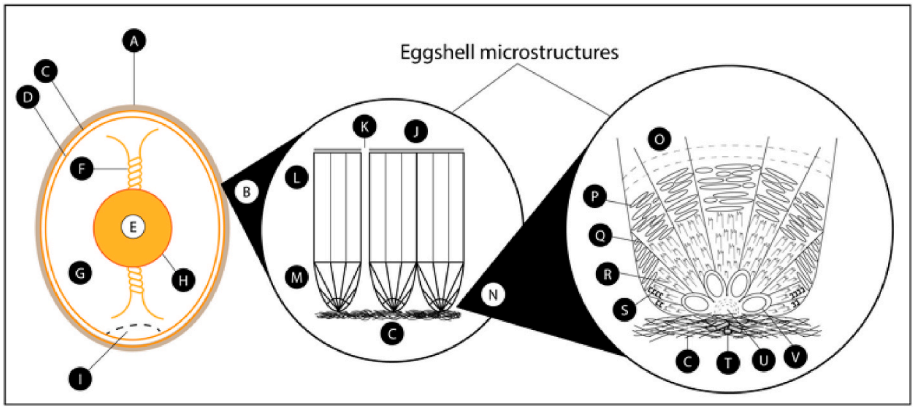

Fig. 1. Anatomy of an avian egg with detail of eggshell interior surface microstructures in radial cross-section: A) eggshell; B) magnified view of eggshell interior surface; C) outer shell membrane (inner surface of eggshell); D) inner shell membrane; E) yolk; F) chalazae; G) albumen; H) vitelline membrane; I) air sac; J) cuticle layer (exterior surface of eggshell); K) pore; L) palisade layer; M) mamillary cone; N) magnified view of mammillary cone; O) wedges (initial stage of growth); P) crystalline cords in the wedges (tabular structure); Q) large radiating organic membranes; R) radiating spicular and prismatic crystallites; S) large plates of fused radial crystallites; T) plates of eisospherite; U) spherite body; V) hole locules. Adapted from (Mikhailov, (1987)).

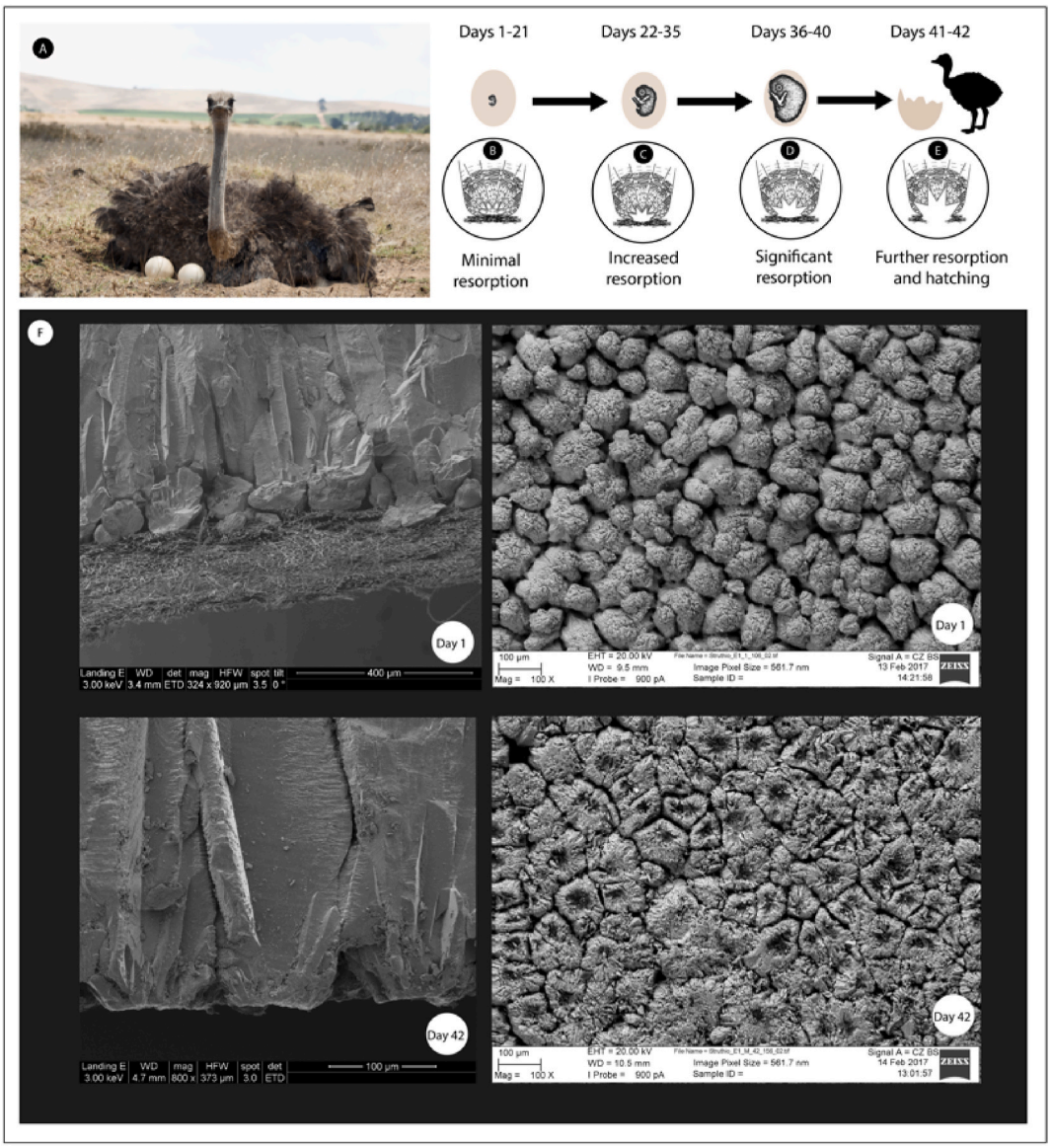

Fig. 2. Eggshell calcium carbonate resorption during the course of incubation and stages of embryonic development and eggshell microstructural changes in Common Ostrich (*Struthio camelus*): A) photo of a female ostrich covering her nest; B) minimal resorption corresponding to "Early" stage in our 3-stage model; C) increased resorption, corresponding to "Middle" stage in our 3-stage model and evidenced by the appearance of pitting of the hole locules and spherite bodies (see Fig. 1 for anatomical detail); D) significant resorption corresponding to "Late" stage in our 3-stage model and evidenced by pitting of the hole locules, spherite bodies, and radiating spicular and prismatic crystallites (see Fig. 1); E) hatching stage, featuring further resorption and also corresponding to "Late" stage in our model; F) 2D SEM images of ostrich eggshell in radial cross-section and top-down view, showing details of mammillary cone resorption at the beginning and end of incubation (days 1 and 42). For full set of 3D image plates showing eggshell changes throughout the incubation window refer to Supp. Fig. 17-Supp. Fig. 23. NB: In the radial cross-section views, the membrane is present on the day 1 sample, revealing its interdigitation with the mammillary cones, and has been removed through a bleach bath on the day 42 sample (see Materials and Methods for eggshell pre-treatment protocol).

instruments and techniques, and evaluate the reliability of qualitative visual inspection of 2D images, as compared to a statistical modeling approach using 3D data.

2. **We test whether our statistical model, derived from an ostrich time series, successfully predicts the ontogenetic age of eggshell of other avian taxa and identify limitations of this proxy approach.** The ability to use ostrich as a model oospecies would greatly expand the utility of these methods to the study of extinct ratite species and extant species for which high-resolution eggshell ontogenetic time series are not available. Generating an ontogenetic time series of eggshell requires sacrificing fertilized eggs with developing embryos and known lay dates. As such, creating the necessary comparative samples is often neither feasible nor ethical for the particular species of interest.
3. **We conduct a sensitivity analysis to test the robustness of our model, providing an approach to the issue of archaeological eggshell diagenesis.** This is particularly important in archaeological contexts where taphonomic factors lead to poor preservation of eggshell remains.

2. Materials and methods

2.1. Sample description

Fragments of eggshell belonging to farm-reared birds of the southern African sub-species of ostrich (*Struthio camelus australis*) were obtained from the Oudtshoorn Research Farm of the Western Cape Government Department of Agriculture, South Africa. These eggshell fragments were

a by-product of ongoing research at Oudtshoorn aimed at reducing levels of reproductive failure (e.g. incidence of dead-in-shell (DIS) chicks) and improving the economic viability of the commercial ostrich production industry (Brand, 2012; Brand et al., 2014; Brand et al., 2017a; Brand et al., 2017b). As a result, eggshell fragments ranging in size from 5 to 10 cm^2 and representing every day (1–42) of embryonic development were obtained from three separate eggs (each from a different hen) for each day (3 eggs × 42 days = total of 126 eggs sampled from 126 hens). Each egg was sampled at four locations on the egg: 1) pole where the air sac was located, 2) opposite pole, 3) equator and 4) opposite side of the equator (Fig. 3). A total of 504 eggshell fragments were thus available for the study and constitute the largest comparative collection of ostrich eggshell of known ontogenetic age and sampling location. The collection is archived in the Olo Be Taloha Lab at Penn State University and available for further study.

For each egg sampled in the collection, the following data were also recorded (see Supp. Table 7) following methods previously reported (Brand et al., 2017a):

- Egg weight at 0 days of incubation
- Egg weight when sampled
- Moisture loss
- Egg length
- Egg width
- Embryo weight (from day 8)
- Embryo length (from day 8)
- Embryo Leg length (from day 8)
- Embryo Beak length (from day 9)
- Embryo Wing length (from day 9)

Export and import were permitted and overseen by the Western Cape Government Department of Agriculture, the University of Pretoria, the Convention on International Trade in Endangered Species of Wild Fauna and Flora (CITES), the US Fish and Wildlife Service, the Smithsonian Institution's National Museum of Natural History and the Pennsylvania State University. In accordance with the US Department of Agriculture's Animal and Plant Health Inspection Service's import requirements, all samples were submerged in 70% alcohol to prevent any potential spread of pathogens.

In addition to samples of ostrich eggshell, samples of Emu (*Dromaius novaehollandiae*; Fig. 11) eggshell of known ontogenetic age were used in this study (Fig. 10). These samples were provided to KD by colleagues who had leftover eggshell samples from separate projects on the embryonic development of this species. The location on the egg from which these samples were collected was not recorded. Sample preparation for emu eggshells was the same as for ostrich eggshells.

2.2. Sample preparation

Eggshell fragments were sub-sampled for SEM, OP and digital microscopy using a Dremel rotary tool fitted with a diamond cutting wheel. Micro-CT sub-samples were cut using a low speed wet saw set to a specified width of 3 mm and fitted with a diamond cutting wheel to minimize splintering of these narrow samples. With the exception of micro-CT samples, all modern eggshell sub-samples were submerged for 25 min in a bath of commercially available bleach to remove the eggshell membrane (Fig. 1) without damaging the mammillary layer (Cusack and Fraser, 2002). Samples were then rinsed in distilled water and air-dried. Micro-CT samples were scanned with the membrane intact, in order to visualize the interaction between the eggshell membrane and the mammillae.

2.3. Scanning electron microscopy

2D secondary electron images were collected using a NanoSEM 630, FEI, Hillsboro, OR, at 3 keV. Cross-section and radial views were taken at multiple magnification levels on 4 equator region eggshell samples representing days 1, 31, 38, 42; see Fig. 2). Samples were coated with a roughly 5 nm layer of iridium.

In addition to generating 2D SEM images, we developed an approach to capture 3D data using a Zeiss EVO low vacuum SEM (3D surface reconstructed on 1 archaeological eggshell fragment of unknown ontogenetic age; see Supp. Fig. 1). Data capture techniques were based on the work of Neffra Matthews and Tommy Noble at the US Bureau of Land Management and further refined by the team at the Cultural Heritage Institute and adapted for use in the SEM. An overlapping tilt series of images were captured from multiple rotational orientations ensuring at least 9 views of every point on the surface of the specimen. Image capture parameters were 20 kV accelerating voltage and 900 pA probe current using a 4 quadrant backscatter detector in composition mode. These images were then processed in Agisoft PhotoScan Pro using Structure From Motion (SFM) algorithms in an iterative process to accurately determine the calibration and pose of the microscope. This produced a set of point correspondences in virtual space representing the surface of the eggshell. Having determined the orientation and pose of the sensor in each image, a Multi-Viewpoint Stereo algorithm was applied to back project the intersection of each pixel in the image to a point in virtual space, thereby generating a dense point cloud upon which a 3D surface was created using MeshLab.

2.4. Micro-CT

One eggshell fragment from the equator and one eggshell fragment from the air sac regions from ostrich eggs representing each day of

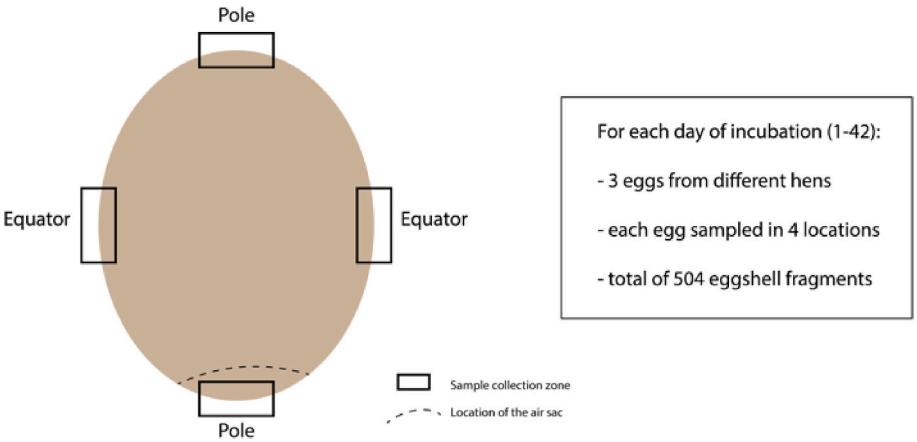

Fig. 3. Ostrich eggshell sampling diagram, showing the location of the air sac, which changes in size during the course of incubation.

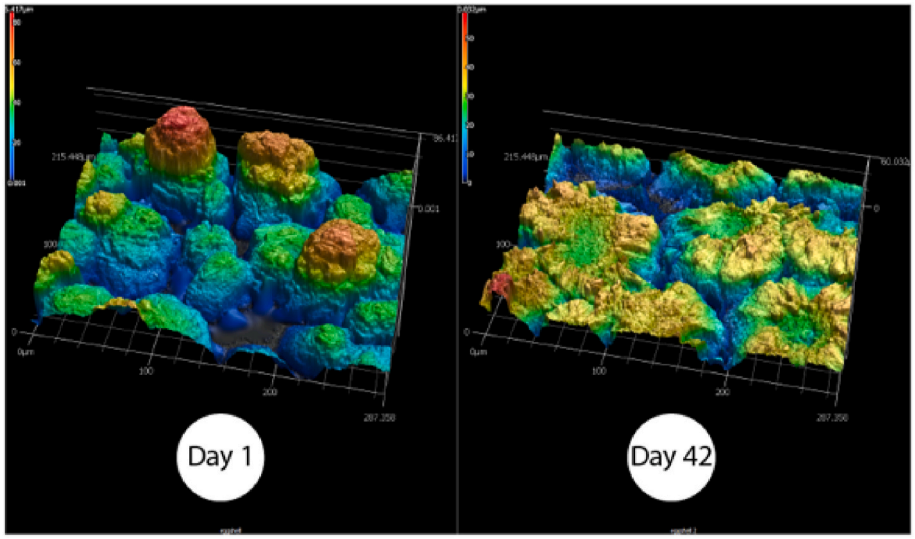

Fig. 4. 3D view of ostrich eggshell mammillary cones at the time the egg was laid (day 1) and at the time of hatching (day 42), showing the degree of resorption of eggshell calcium carbonate over the full incubation period. Data collected using a Keyence VK-X (violet) laser scanning digital microscope. See Supp. Fig. 17-Supp. Fig. 23 for 3D images representing each day of incubation.

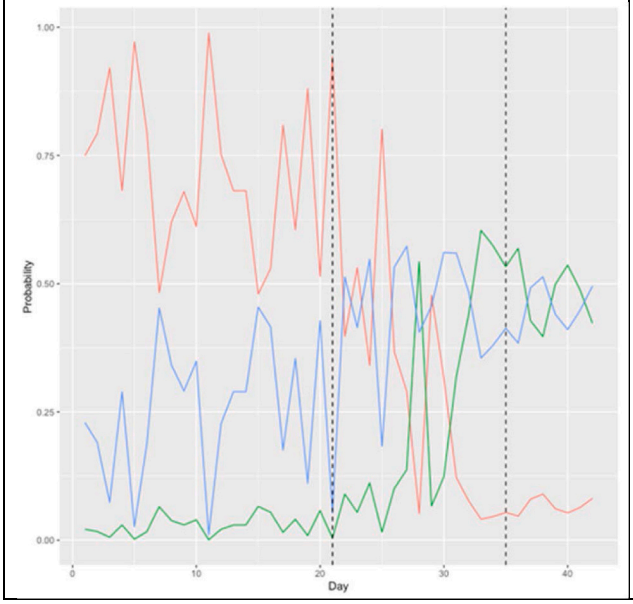

Mis-classification matrix

Predicted Sampling Stage	True Sampling Period		
	Early	Mid	Late
Early	**21**	3	0
Mid	0	**7**	3
Late	0	4	**4**
Total Number of eggs	21	14	7
Classification accuracy (%)	100 %	50%	57%

Fig. 5. Comparison of Predicted and True Sampling Period (One-Predictor Model) with eggs discretized into 3 stages (Early, Middle and Late). The left side of the figure is a visual summary of the predicted sampling stage probabilities for the 42 eggs in the testing set, where the colored lines reflect the marginal probability values for "Early" (red), "Middle" (blue) and "Late" (green) stages. The right side of the figure is a summary of the model's success rate (mis-classification matrix). Boldfaced numbers in the shaded cells of the matrix are the correct classifications. (For interpretation of the references to color in this figure legend, the reader is referred to the Web version of this article.)

incubation (2 samples per egg x 1 egg per day x 42 days; n = 84) were CT-scanned at beamline 2-BM at the Advanced Photon Source facility at the U.S. Department of Energy's Argonne National Laboratory (Argonne, IL). Samples were mounted to a post using modeling clay. Scans were made with an exposure time of 100 ms at 27.4 keV to acquire 1500 projections as the sample rotated 180° at $3^{\circ}s^{-1}$ (Supp. Fig. 2 and Supp. Fig. 3). Datasets were reconstructed as TIFF image stacks using the TomoPy Python package (https://tomopy.readthedocs.io) in Linux on a Dell Precision T7610 workstation with two Intel Xeon processors yielding 16 cores, 192-GB RAM, and NVIDIA Quadro K6000 with 12-GB VRAM. The isotropic voxel dimensions of the image stacks were 0.65 μm and the field of view of each data set was ~1.5 mm^3.

2.5. Optical profilometry

One eggshell fragment from the equator region from ostrich eggs representing each day of incubation (1 sample per egg x 3 eggs per day x 42 days; n = 126) were imaged using optical profilometry. Optical profilometry data were collected on a Zygo Nexview 3D system (Zygo-Ametek Corp, Middlefield, CT). Surface scans were performed in CSI mode with HDR enabled. The 50× objective (0.55 NA, Zygo-Ametek Corp.) with an internal magnification of 0.5X was used to collect

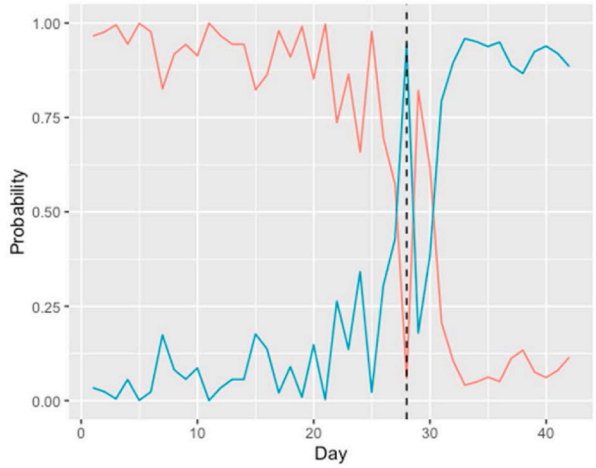

Mis-classification matrix		
Predicted Sampling Stage	True Sampling Period	
	Early	Late
Early	**27**	2
Late	1	**12**
Total Number of eggs	28	14
Classification accuracy (%)	96%	86%

Fig. 6. Comparison of Predicted and True Sampling Period (One-Predictor Model) with eggs discretized into 2 stages (Early and Late). The left side of the figure is a visual summary of the predicted sampling stage probabilities for the 42 eggs in the testing set, where the colored lines reflect the marginal probability values for "Early" (red) and "Late" (green) stages. The right side of the figure is a summary of the model's success rate (mis-classification matrix). Boldfaced numbers in the shaded cells of the matrix are the correct classifications. (For interpretation of the references to color in this figure legend, the reader is referred to the Web version of this article.)

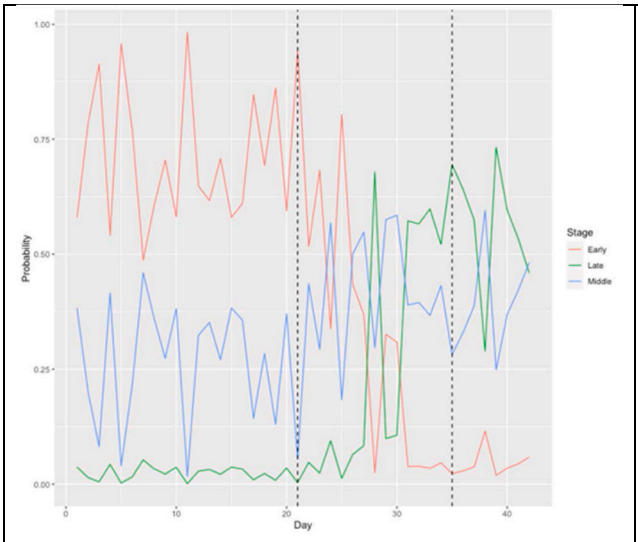

Mis-classification matrix			
Predicted Sampling Stage	True Sampling Period		
	Early	Mid	Late
Early	**21**	3	0
Mid	0	**5**	2
Late	0	6	**5**
Total Number of eggs	21	14	7
Classification accuracy (%)	100%	36%	71%

Fig. 7. Comparison of Predicted and True Sampling Period (Four-Predictor Model). The left side of the figure is a visual summary of the predicted sampling stage probabilities for the 42 eggs in the testing set, where the colored lines reflect the marginal probability values for "Early" (red), "Middle" (blue) and "Late" (green) stages. The right side of the figure is a summary of the model's success rate (mis-classification matrix). Boldfaced numbers in the shaded cells of the matrix are the correct classifications. (For interpretation of the references to color in this figure legend, the reader is referred to the Web version of this article.)

individual scans, with a Z scan between 100 and 200 μm. A 4x4 stitching routine with 20% overlap was used to collect an image of the surface with a 1.1 mm field of view (Supp. Fig. 4). Data analysis was done with Zygo's Mx software. A surface plane form remove was applied to the images prior to surface parameter calculations.

2.6. Laser scanning confocal microscopy

Scans of 2 equator region eggshell fragments representing days 1 and 42 were acquired using a Keyence VK-X1100 (violet) 3D laser scanning microscope (Fig. 4). Auto mode, which automatically determines the Z range of the sample as well as the necessary laser intensity, was used to collect the data. The average Z range was 0.5 nm and the average XY range was 130 nm. The raw data were then processed using the VK-X1100 software. The surface shape correction tool was applied to normalize the surface, to reduce variation caused by the differential curvature of each sample. Surface roughness measurements were generated using the area roughness tool in the VK-X1100 software.

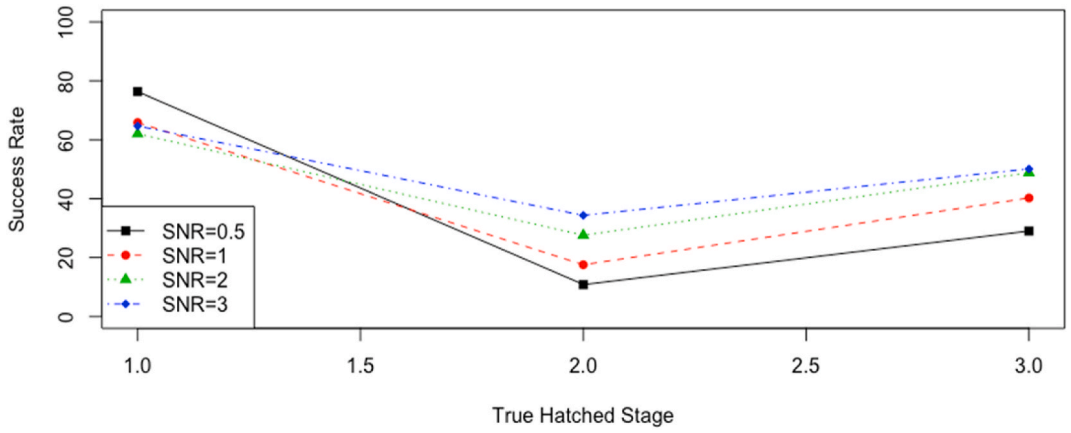

Fig. 8. Graphical summary of sensitivity analysis showing the variability in the classification success rates with the addition of different amounts of error.

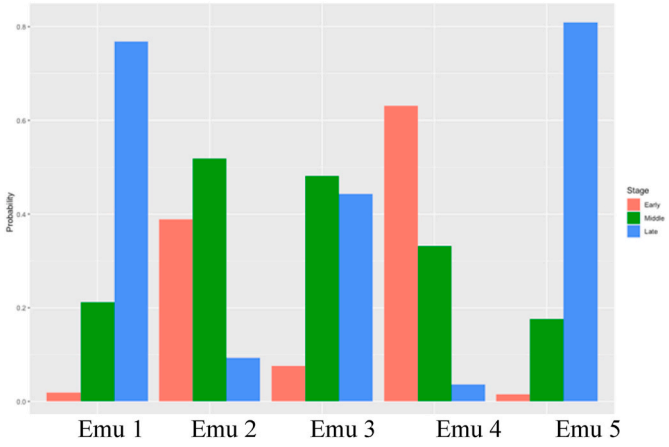

Fig. 9. Predicted sampling stage probabilities for emu eggshell samples.

2.7. Digital microscopy

Scans of equator region eggshell fragments representing days 1 and 41 were acquired using a Keyence VHX-7000 laser scanning digital microscope, which renders a 3D surface through depth-of-field calculations. Modern *Struthio* eggshell fragments were stained, in order to reduce surface reflectance and improve the resolution of 3D surface renderings. Samples were stained for 10 min with 0.3 mg/ml Toluidine Blue (Fisher, T161-25) in dH2O on a rocking platform and then removed and cleaned with dH2O for less than 1 min before being left to air dry. Data were acquired at 400× magnification using the fine depth composition feature to render a high-resolution 3D image. A 1 × 1mm area on each sample was scanned using the automatic stitch function (Supp. Fig. 5). Surface roughness measurements were generated using the area roughness tool in the VHX-7000 software.

2.8. Statistical analyses

Using 3D optical profilometry scans of the ostrich eggshell comparative collection (Supp. Fig. 17-Supp. Fig. 23), we developed and compared the success rates of two predictive models. Each model generates a prediction of eggshell ontogenetic age based on surface roughness measurements taken on the interior portion of eggshell samples from the equator region. Equator fragments were selected instead of pole region fragments, since micro-CT and SEM scans revealed that the air sac shields the eggshell from resorption, thus obscuring the developmental process we aimed to observe (see Supp. Fig. 6). For developing our models, we selected common surface roughness parameters (S2), based on correlations between parameters (Supp. Fig. 11), namely Sa (arithmetic mean height; Supp. Fig. 7), Sku (kurtosis; Supp. Fig. 8), Ssk (skewness; Supp. Fig. 9), and Sz (maximum height; Supp. Fig. 10). We developed a one-predictor model (with Sa as the only predictor variable) and a four-predictor model (with Sa, Sku, Ssk, Sz as predictors).

In the collected data, the outcome is the number of days from the time an egg was laid (day 1) until the egg hatched (day 42) or was

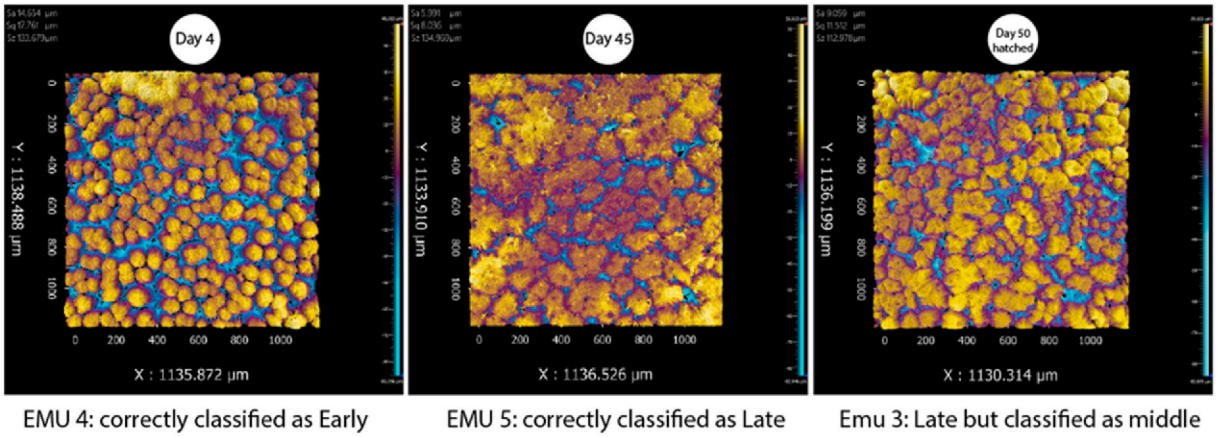

Fig. 10. 3D views of emu eggshell samples, showing their mamillary cones, their ontogenetic age and results of their classification by our one-predictor, 3-stage model. Data collected using a Zygo Nexview 3D optical profilometer.

harvested prior to hatching and broken open for sampling (days 1–41). Prior to developing our statistical models, we discretized the outcome variable (days to sampling or hatching) as "Early" (from day 1 to day 21), "Middle" (from day 22–35) and "Late" (day 36–42). These three stages were established based on detailed observations of embryonic growth in ostriches (Brand et al., 2017a). The three time bins/stages of our models follow the exponential rate of weight increase of the developing embryo, which we use as a proxy for an increase in energetic demands and thus expected rate of eggshell resorption (see Table 2). In the "Early" stage, weight increases slowly, followed by more rapid weight increase in the "Middle" stage and an increase in weight ranging from 29% to 64% in the "Late" stage. Samples derived from eggs from which a chick hatched are included in our "Late" stage bin as there is no clear trend distinguishing roughness measurements taken on eggs sampled on days 36–40 versus those sampled or hatched on days 41–42 (Supp. Fig. 24-Supp. Fig. 31). For our one-predictor model we also ran an analysis with the outcome variable (days to sampling or hatching) discretized into 2 time bins/stages, "Early" (days 1–28) and "Late" (days 29–42). We observed a pronounced flattening of mammillary cones around days 28–29 in our visual inspection of the time series, and previous research suggests this period corresponds to the beginning of bone ossification and a resultant increase in Ca absorption (Table 2).

Ontogenetic age ("Early", "Middle" or "Late) was then integrated with the roughness measurements through an ordinal logistic regression model (Agresti, 2013). Such a model allows us to investigate how well the roughness measurements predict the ontogenetic age of the eggs. Since roughness measurements were available for three eggs on each of the 42 days of development, we picked two eggs from each day as the training set and one egg from each day as the testing set. We developed the predictive models using the training set and later used the testing set as a diagnostic tool to check the goodness-of-fit of the models. We used the "*plor*" package in *R* to perform the ordinal logistic regression (S4).

2.9. Notation and model setup

Our predictive models are described using the following notation: Y is the ordered response with J categories. $P(Y \leq j|x)$ is the probability that Y is less than or equal to the j^{th} category for a given value of $\boldsymbol{x}$, in which x represents the predictor variables in the model. The odds of the response being less than or equal to a particular category is defined as

$$\frac{P(Y<j|x)}{P(Y>j|x)}$$

Then the cumulative log odds are defined as

$$\log it(P(Y \leq j|x)) = \log\left(\frac{P(Y<j|x)}{P(Y>j|x)}\right) = \log\left(\frac{P(Y \leq j|x)}{1-P(Y \leq j|x)}\right), j = 1, 2, ...J-1$$

We modeled the cumulative log odds as a function of the explanatory variables through a cumulative logit model. In particular, the cumulative logit model for these data is written as

$$\log\left(\frac{P(Y \leq j|x)}{P(Y>j|x)}\right) = \alpha_j + \boldsymbol{\beta^T x}, j = 1, 2, ...J-1.$$

In the above model.

- $Y = \begin{cases} 1 \textit{ if sampled during the early stage } (\textit{days } 1-21) \\ 2 \textit{ if sampled during the middle stage } (\textit{days } 22-35) \\ 3 \textit{ if sampled during the late stage } (\textit{days } 36-42) \end{cases}$
- $J = 3$ for three categories of the response: early, middle and late.
- $\log\left(\frac{P(Y \leq j|x)}{P(Y>j|x)}\right)$ is the log odds of an egg being sampled at a certain stage or earlier for a given value of the predictor variable(s)
- α_j is the intercept for each cumulative logit
- $\beta = (\beta_1, \beta_2, ...\beta_p)^T$ is a vector of regression coefficients corresponding to the roughness measurements

Parameter estimates and the standard errors are estimated using the *plor* package in *R* (Table 1; Supp. Table 6). Since the *plor* package does not produce p-values to test the significance of the roughness parameters, approximate p-values were obtained by comparing the *t*-test statistic with corresponding standard normal percentiles (Table 1; Supp. Table 6).

The one-predictor model (using Sa as a variable) can be written as

$$\begin{aligned} \log it\left(\widehat{P}(Y \leq 1)\right) &= -7.44 + 0.54Sa \\ \log it\left(\widehat{P}(Y \leq 2)\right) &= -4.71 + 0.54Sa \end{aligned} \quad (1)$$

Then the model parameters are interpreted as:

- For every unit increase in Sa, the odds of an egg being sampled during the early stage of its incubation (as opposed to middle or late stages) is expected to increase by 71.6% ($e^{0.54} = 1.\mathbf{716}$)
- The odds of an egg being sampled during the early stage (as opposed to middle or late stages) is expected to be 0.0006 ($e^{-7.44} = 0.0006$) when Sa is equal to zero
- The odds of being sampled during the early or middle stages (as opposed to late stage) is expected to be 0.009 ($e^{-4.71} = 0.009$) when Sa is equal to zero

The numerical values we obtained for the model parameter estimates agree with our initial observations of the relationship between eggshell ontogenetic age and the Sa roughness measurement (S2), in which higher Sa values are associated with early stages of the incubation period (Supp. Fig. 12 and Supp. Fig. 13).

The four-predictor model (using Sa, Sku, Ssk, Sz) can be written as

$$\begin{aligned} \log it\left(\widehat{P}(Y \leq 1)\right) &= -4.57 + 0.40Sa - 0.10Sku + 1.17Ssk + 2.14 \times 10^{-5}Sz \\ \log it\left(\widehat{P}(Y \leq 2)\right) &= -1.64 + 0.40Sa - 0.10Sku + 1.17Ssk + 2.14 \times 10^{-5}Sz \end{aligned} \quad (2)$$

See Supp. Table 6 for estimated model parameters and the corresponding p-values.

2.10. Sensitivity analysis

We conducted a sensitivity analysis to test the robustness of our one-predictor, 3-stage model, since our ultimate goal is to develop methods that are appropriate for the analysis of fossilized eggshell that has been impacted by taphonomic factors and may feature differential preservation of microstructures. To account for the additional variability in the surface roughness of fossilized eggs, we conducted a sensitivity analysis by adding a random error to the ostrich eggshell data and assessing the prediction from the one-predictor model with a predefined signal-to-noise ratio (SNR). Steps for the sensitivity analysis are summarized below.

Step 1: The mean signal was calculated by taking the average of the Sa values of the three eggs for each of the 42 days.

Step 2: The standard deviation was calculated for a predefined SNR value, in which $SNR = \frac{\overline{x}}{\sigma_e}$, where $\overline{x}$ is the average *Sa* on a given day and σ_e is the standard deviation of the error distribution (Welvaert and Rosseel,

Table 1
Parameter estimates from one-predictor model.

Variable	Coefficient	Standard Error	Approximate p-values
Sa	−0.5448	0.0999	4.98×10^{-8}
1|2	−7.4422	1.3933	9.23×10^{-8}
2|3	−4.7079	1.1137	2.37×10^{-5}

Note: R parameterization of the ordinal logistic model is.$\log it(P(Y \leq j|x)) = \alpha_j - \eta^T x. j = 1, 2, ...J-1$

Table 2
Summary of key stages of ostrich embryonic development and their relationship to changes in eggshell morphology.

		Source*	Days of incubation: 1 2 3 4 5 6 7 8 9 10 11 12 13 14 15 16 17 18 19 20 21 22 23 24 25 26 27 28 29 30 31 32 33 34 35 36 37 38 39 40 41 42
Previous Research	Ca absoprtion*	1,2	Calcium absorbed from yolk | Calcium absorbed from eggshell as bones begin to ossify
	Eggshell microstructure*	1	No detectable changes | initial flattening of mammillary cones | pitting of cones | further flattening of mammillary cones (erosion of pit walls)
	Description of Ostrich Embryo	3,4,5	A | B | C | D | E | F
	Embryo Weight (g)	3, T1	0.17 ± 0.15 | 2.78 ± 0.23 | 21.0 ± 0.83 | 156 ± 4.73 | 399 ± 11.9 | 910 ± 31.1
	Albumen Weight (g)	3, T1	691 ± 18.8 | 432 ± 16.4 | 481 ± 18.7 | 273 ± 19.8 | 181 ± 38.2 | -
	Yolk Weight (g)	3, T1	366 ± 21.9 | 614 ± 18.6 | 575 ± 20.5 | 634 ± 20.2 | 550 ± 20.9 | -
This paper	Ostrich eggshell microstructure	6	no detectable changes | initial flattening of mammillary cones | pitting of cones | further flattening of mammillary cones (erosion of pit walls)
	Roughness measurments	6	initial changes | pronounced change
	3-Stage model	6	Early | Middle | Late
	Classification accuracy	6	100% | 50% | 57%
	2-Stage model	6	Early | Late
	Classification accuracy	6	96% | 86%
	Egg composition	4	Yolk + Albumen (embryo weighs less than albumen) | Yolk + Embryo (embryo weighs more than albumen) | Full-term chick

*Sources: 1 (Chien, et al., 2009); 2 (Bellairs and Osmond, 2014); 3 (Brand, 2012); 4 (Brand, et al., 2017a); 5 (Ar and Gefen, 1998); 6 (this paper).
**Based on embryonic studies of chicken (Gallus gallus). Table indicates possible timing of these changes in ostriches (Struthio camelus) estimated by multiplying the time frame observed in chickens, whose incubation period of 21 days is half that of ostriches, by 2.
***Description of ostrich embryo: A – tail bud curved; B – beak, wings and legs present; C – feathers appear; D – claws appear; E – thick coat of feathers, yolk sac retracted halyway into abdominal cavity; F – fully grown, yolk sac retracted into abdominal cavity, all of albumen used.

2013). We carried out the sensitivity analysis for SNR values 0.5, 1, 2 and 3. Smaller SNR values are associated with higher error variability. For instance, when the SNR is fixed at 0.5, σ_e is twice as large as the signal.

Step 3: Error components were generated for each day from normal distributions with a mean of zero and standard deviation determined by the above SNR values.

Step 4: After adding the random error, we obtained a prediction of the ontogenetic age of the egg using the one-predictor model. This was repeated 500 times while discarding the instances in which adding the random error resulted in a negative Sa value.

Step 5: Based on these 500 iterations, success rates (correct classifications) were calculated for each SNR value.

2.11. Visual inspection

Optical profilometry images of a sample of ostrich eggshell representing one egg per day of development (42 samples total) were discretized as "Early" (days 1–21), "Middle" (days 22–35) or "Late" (days 36–42) stage of embryonic development (as described in the previous section) and visually assessed by 3 separate analysts. Each of the 3 analysts have expert knowledge of the process of morphological change in ostrich eggshell during embryonic development but did not know the true ontogenetic age of the samples.

3. Results and discussion

3.1. Comparison of imaging methods

All imaging methods successfully generated high-resolution 3D data of eggshell microstructures. Data capture and processing are quickest using the Keyence VK-X laser scanning confocal microscope (1–3min per sample), followed by the Keyence VHX-7000 digital microscope (3–6min per sample) and Zygo Nexview 3D optical profilometer (20min scan time + 10min postprocessing per sample). All three of these instruments operate with proprietary software packages that generate surface roughness measurements using surface area analysis tools.

Micro-CT scanning creates highly resolved scans of eggshell that can be manipulated in a variety of ways for visualization and quantification of eggshell micro-structures. The advantage of micro-CT data is that they enable analysis through layers of eggshell and there are infinite possibilities for the orientation of cross-sectional views. Data collection was approximately 3h for micro-CT scanning (10–15min scan time + 2.5 h for postprocessing). The primary drawback of micro-CT scans of eggshell is that automatic segmentation of the scans does not generate a faithful reconstruction of the 3D surface, due to similarities in material density across the eggshell surface.

SEM generates high-resolution 2D imagery. 2D SEM scans of eggshell microstructures can be used for visual inspection of mammillary cone resorption, as demonstrated in previous studies (e.g. Beacham and Durand, 2007). 2D SEM data collection was approximately 1–2mins per scan. The tilt-series method generates equally high-resolution 3D surfaces of eggshell, but data capture (~1hr) and postprocessing time (~1hr) are greater than the laser and digital microscopy and

profilometry approaches. SEM instruments, however, may be more widely available to researchers and eggshell surface 3D point cloud data can be exported and analyzed using open-source software packages (S2).

3.2. Ostrich eggshell developmental series

Detailed descriptions of the stages of embryonic growth in ostrich have been previously reported (Brand et al., 2017a; see Table 2). Here we describe changes in eggshell morphology, including surface textures, and link these changes to observations of embryonic growth. We include data pertaining to equator eggshell fragments in our ostrich eggshell developmental series (3 eggs × 42 days: n = 126), including surface texture measurements, and measurements pertaining to the complete egg from which the fragments were derived, as well as the embryo that was either sacrificed or hatched from the egg (Supp. Table 7). We also provide a 3D image of the interior surface of one ostrich equator region eggshell fragment from our developmental series for each day of development (days 1–42; see Supp. Fig. 17-Supp. Fig. 23).

We observed that ostrich eggshell samples in our developmental series vary in terms of the size, density and clustering of mamillary cones and pores (Supp. Fig. 17-Supp. Fig. 23). Mammillary cones range between ~20 and 200 μm in diameter and can reach close to 200 μm in height prior to resorption. In some samples, the size of cones is relatively uniform, as compared to other samples, where there is a diversity of cone sizes (e.g. Supp. Fig. 21, "Day 25" vs. "Day 26"). Variability was also observed with regard to the density of cones and their spatial distribution (e.g. degree of clustering).

Changes in eggshell microstructures are visible in 3D images of eggshell surfaces (Supp. Fig. 17-Supp. Fig. 23) beginning on day 26, when we note a slight flattening of mammillary cone peaks (Supp. Fig. 21). This visible change in cone structure corresponds to a window of rapid embryonic growth (days 21–28), in which the length of the embryo increases by 81%, its weight exhibits a 7-fold increase and leg length doubles (Brand et al., 2017a; p. 141). Between days 28 and 30, we observe a more pronounced flattening of mammillary cones, followed by the appearance of pitting at the top of the cones as early as day 28 (Supp. Fig. 21), but more consistently by day 31 (Supp. Fig. 22). By day 33 pits widen and get deeper (Supp. Fig. 22-Supp. Fig. 23). During the last four days of incubation (days 39–42) the size of pits does not noticeably change, but we observe a significant flattening of mammillary cones. These changes fall withing the last week of incubation, in which the weight of the embryo increases from 29% to 64% of initial egg weight (Brand et al., 2017a; p. 141).

We calculated Pearson's correlations to assess the relationship between eggshell ontogenetic age in days and surface roughness measurements Sa, Sku, Ssk and Sz (Table 3; Supp. Fig. 24-Supp. Fig. 31). These correlations were all significant at the 0.01 level (2-tailed). The strongest relationship observed was between eggshell age and Sa (Supp. Fig. 7). There was a high negative correlation between these variables, though it should be noted that only roughly 50% of the variation in Sa values can be explained by eggshell age ($R^2 = 0.5196$; Supp. Fig. 24). This meets our expectation that as the embryo develops and draws nutrients from the shell, the mean height of the mammillary cones decreases. The decrease in Sa values is most pronounced beginning on day 29 of incubation (Supp. Fig. 24 and Supp. Fig. 25), immediately following the rapid period of growth between days 21–28 described above.

The relationship between eggshell age and Sku (Supp. Fig. 8) was highly positively correlated (Table 3; Supp. Fig. 26-Supp. Fig. 27). As the embryo develops, the sharpness of eggshell surface microstructures thus increases. The increase in Sku values is most pronounced beginning on day 30, which also closely follows the period of rapid growth between days 21–28 (Supp. Fig. 26-Supp. Fig. 27).

The relationship between eggshell age and Ssk (Supp. Fig. 9) was highly negatively correlated (Table 3), indicating that as the incubation period progresses, the height distribution of peaks and pits on the interior eggshell surface goes from being roughly symmetrical to being skewed above the mean plane. The decrease in Ssk values is also most pronounced beginning on day 30 (Supp. Fig. 28-Supp. Fig. 29).

We observed a weaker relationship between eggshell age and Sz. These variables were negatively correlated (Table 3), indicating that maximum peak heights and pit depths decrease over the course of incubation (Supp. Fig. 30-Supp. Fig. 31).

We also calculated Pearson's correlations to assess the relationship between egg and embryo measurements, and eggshell surface roughness measurements (Table 4-Table 5). Relationships between egg measurements and surface roughness were weaker overall than the relationships between embryo measurements and surface roughness. This indicates that changes in eggshell interior surface microstructures are most highly correlated with changes linked to growth of the embryo.

3.3. Predictive modeling of eggshell ontogenetic age

Based on the one-predictor, 3-stage model described by Equation (1), we obtained the marginal sampling date probabilities for each egg in our testing set. For each of the 42 eggs, the model estimates the probability that the egg was sampled during the "Early", "Middle" and "Late" stages of development. The predicted ontogenetic age is thus the sampling date with the highest marginal probability. For instance, for the egg that was sampled on day 1 in the testing set (Supp. Table 2), the predicted probabilities of being sampled in the "Early", "Middle" and "Late" stages are 0.75, 0.23 and 0.02 respectively. Based on these probabilities, the predicted ontogenetic age of the egg is "Early" (e.g. days 0–21).

Using the one-predictor, 3-stage model, all 21 eggs that were sampled in the "Early" stage were correctly classified (Fig. 5). The success of the model at predicting the age of "Early" stage eggs is evidenced by the dominance of the "Early" probability from days 0–21 (red line, Fig. 5). The model was less successful in its classification of "Middle" and "Late" stage eggs, which were correctly classified 50% and 57% of the time, respectively. "Middle" stage eggs are misclassified both as "Early" and as "Late" stage eggs, which is clear from the alternating dominance of the "Early" and "Late" probabilities from days 22–35 (red and green lines, Fig. 5). "Late" stage eggs were never misclassified as "Early", but were misclassified as "Middle" stage, as evidenced by the alternating dominance of the "Late" and "Middle" probabilities from days 36–42 (green and blue lines, Fig. 5).

Unsurprisingly, the overall accuracy of the predictions was higher using the one-predictor, 2-stage model (Fig. 6). In this iteration of the

Table 3
Pearson's r values reflecting correlations between eggshell ontogenetic age and surface roughness measurements.

	Sa	Sku	Ssk	Sz
Eggshell age in days	-0.72	0.64	-0.61	-0.43
Number of observations	126	126	126	126

*The darker the blue shading the more linearly correlated the variables are; the darker the red shading, the more negatively linearly correlated the variables are.

Table 4
Pearson's r values reflecting correlations between roughness parameters included in our predictive model and egg measurements.

	Egg weight on lay date	Egg weight on date sampled	Egg length in mm	Egg width in mm
Sa	0.03	0.39	-0.13	0.21
Sku	0.03	-0.32	0.03	-0.11
Ssk	0.02	0.33	-0.08	0.16
Sz	0.66	0.25	-0.16	0.19
Number of observations	126	126	126	126

*The darker the blue shading the more linearly correlated the variables are; the darker the red shading, the more negatively linearly correlated the variables are.

Table 5
Pearson's r values reflecting correlations between roughness parameters included in our predictive model and egg measurements.

	Embryo weight on date sampled	Embryo length on date sampled	Leg length in mm	Beak length in mm	Upper wing length in mm	Lower wing length in mm	Wing length in mm
Sa	-0.72	-0.78	-0.78	-0.48	-0.71	-0.74	0.39
Sku	0.69	0.69	0.70	0.42	0.60	0.70	-0.68
Ssk	-0.66	-0.73	-0.73	-0.47	-0.64	-0.72	-0.37
Sz	-0.52	-0.56	-0.55	-0.21	-0.51	-0.51	0.25
Number of observations	105	105	105	97	96	96	6

*The darker the blue shading the more linearly correlated the variables are; the darker the red shading, the more negatively linearly correlated the variables are.
**When embryo measurements were not available (e.g. when a morphological feature had not emerged or was too small to be accurately measured), we omitted those samples from the calculation, such that in some cases fewer observations were included than the total samples in the ostrich series (n=126; refer to Supp. Table 7).

model, "Early" stage eggs were successfully classified 96% of the time, while "Late" stage eggs were correctly classified 86% of the time. The marginal probabilities that an egg is in the "Early" vs. "Late" stage are generally clearly distinguished, as evidenced by the dominance of the red line to the left of the dashed line and the dominance of the green line to the right of the dashed line. The clear dominance of the probability that an egg is "Early" or "Late" holds throughout the time series, except between days 27 and 30, when the marginal probability lines intersect (Fig. 6). These four days are when we observe the initial flattening of mamillary cones and is right before pitting is visible (Table 2).

The four-predictor model, in which roughness measures Sa, Sku, Ssk, Sz were included as predictors, yielded similar results to the one-predictor model (Fig. 7). "Early" stage eggs were always correctly classified and "Middle" stage eggs were misclassified as both "Early" and "Late" stage. The primary difference in the success rates of the four-predictor model is that "Late" stage eggs were classified correctly at a higher rate (71%) than with the one-predictor model (57%). This is evidenced by the differences between the predicted probabilities from days 36–42, where the "Late" probability line (green) is dominant more frequently and in a more pronounced fashion (Fig. 7).

Finally, we report the range between the first and third quartiles for each roughness measurement—Sa, Sku, Ssk and Sz—for our developmental series with eggs discretized as being in the Early, Middle or Late stage of development (Supp. Fig. 12-Supp. Fig. 16 and Supp. Table 1-Supp. Table 4). These ranges can inform preliminary analysis of eggshell fragments of unknown ontogenetic age.

Table 6
Tabular summary of sensitivity analysis showing the variability in the classification success rates with the addition of different amounts of error.

Stage	Success Rate			
	SNR = 0.5	SNR = 1	SNR = 2	SNR = 3
Early (1)	76%	66%	62%	64%
Middle (2)	11%	18%	28%	34%
Late (3)	29%	40%	49%	50%

3.4. Sensitivity analysis

Results from the sensitivity analysis are summarized in Table 6 and in Fig. 8. As expected, the classification success rates tend to decrease as the error variability increases. However, the success rate in classifying early stage eggs remains relatively high when SNR = 0.5. We expected the success rate to be higher when the SNR is high (meaning there is a stronger signal compared to the noise), however, in the "Early" stage we also observed an unexpected decrease in the success rate of the model when we increased the SNR from 0.5 to 1. This could be due to chance or to the fact that the introduced noise made the differences in "Early" stage eggshell roughness measurements more pronounced. As with the original data, the success rate with different SNRs is lowest for eggs sampled during the "Middle" stage. At the same, "Middle" stage eggshell experienced the biggest increase in the success rate with progressively larger SNRs. These results underscore the need for caution in interpreting roughness measurements derived from archaeological eggshell that has been subjected to taphonomic processes (Hawkins et al., 2019), but suggest the approach can be meaningfully applied to the archaeological record. The classification success rates obtained through this sensitivity analysis provide a guideline for interpreting results of the model when applied to archaeological samples. The success rates using a SNR = 0.5 are the most conservative we obtained and thus most appropriate for relatively weathered samples in an assemblage. Further experimental research is needed to fully characterize the effects of diverse depositional environments on avian eggshell.

In the case of archaeological eggshell assemblages, we recommend noting whether the mammillary cones are visible, and, if so, whether pitting has begun. Even in cases where archaeological eggshell has been subjected to significant post-depositional erosion, the mammillary cones and presence of pitting may be identifiable (see Supp. Fig. 1). For ostrich eggshell, the presence of pitting at the top of the mammillary cones is a certain indication that the egg and embryo developed until at least day 28 (see section 3.2; Supp. Fig. 21), a developmental stage that corresponds to a period of rapid embryonic growth and increased nutrient demands. Archaeological eggshell that displays pitting of the mammillary cones thus contained an embryo that, at a minimum, presented with fully-formed limbs, beak, and claws (Table 2). Depending on the research question, a simple assessment of the presence or absence of mammillary cone pitting may be sufficient.

3.5. Other avian taxa

Eggshell samples of known ontogenetic age assigned emu (*Dromaius novaehollandiae; n = 5*) were also analyzed using the four-predictor, 3-stage model that we developed using the ostrich eggshell series. It is important to emphasize that Emu egg incubation is longer than that of ostrich (50–56 days vs. 42 days), so our model's assumptions about days and stages of incubation are not perfectly aligned with emu development. The model was moderately successful at predicting the age of emu eggshells (60% success rate; Table 7; Fig. 9). In the two cases in which the model's prediction was incorrect (samples E2, E3), the model underestimated the age of two "Late" eggshells and classified them as "Middle" stage. It should be noted that with regard to sample E3, the model probabilities for "Middle" and "Late" were very close (Fig. 9). These results suggest that our ostrich model may be useful for the analysis of eggshells belonging to closely related taxa with comparable incubation windows and developmental stages to ostrich, such as other ratites (Fig. 11). On the other hand, eggshells belonging to more distantly related avian taxa with significantly shorter or longer incubation windows and different developmental trajectories than those of ostriches are likely to require the development of taxon-specific models.

Table 7
True and predicted ages of emu eggshell samples.

Sample ID	True age	Predicted age
Emu 1	Late	Late
Emu 2	Late	Middle
Emu 3	Late	Middle
Emu 4	Early	Early
Emu 5	Late	Late

3.6. Classification of eggshell ontogenetic age through visual inspection

The rate of successful classification of eggshell images according to developmental stage varied across the 3 analysts as well as across the 3 stages of development ("Early", "Middle" and "Late"). Analysts 1 and 3 achieved the same rate of success for "Early" and "Middle" stage eggshells (Table 8). Analyst 3 classified all "Early" and "Late" stage eggshells correctly but achieved the lowest success rate (along with Analyst 1) for "Middle" stage eggshells. Overall, all analysts had greater success correctly classifying "Early" and "Late" stage eggshells, while "Middle" stage eggshells were more frequently misclassified, with greater variability between analysts' classifications, a result consistent with the variable success rates of the predictive models.

At the beginning of the "Middle" stage (day 22), there is an overall tendency to underestimate the ontogenetic age of the eggshells by classifying them as "Early", while in the latter half of the "Middle" stage (beginning ca. day 28) there is a tendency to overestimate the ontogenetic age of the eggshells by classifying them as "Late" (Fig. 12). This suggests that early microstructural changes in eggshell morphology are difficult to detect through visual inspection, and may not be detectable or significant regardless of analytical approach. Beginning approximately at day 28, there appears to be a threshold at which microstructural changes become evident during visual inspection. Once microstructural changes become evident, however, it remains difficult for the analyst to visually distinguish degrees of morphological change, such that once changes are detected, analysts tend to classify eggs as "Late" stage.

3.7. Additional observations regarding eggshell microstructural changes

As described in section 3.2, we observed a correlation between a substantial increase in ostrich embryo weight and the final phase of mammillary cone erosion between days 35–42 of development (Table 1-S8). This suggests that the rate of eggshell calcite resorption is linked to the rate of embryonic growth, and that neither is a perfectly linear time-dependent process. Brand et al. report, for example, that the leg length of ostrich embryos increases by nearly 30% during the late stage of incubation (Brand et al., 2017a). Differences in growth rates between altricial and precocial species (Karlsson and Lilja, 2008; Chinsamy-Turan et al., 2020) suggest that eggshell calcite resorption rates may also differ substantially across different species.

Low hatching rates and problems that occur during commercial poultry farming present challenges for the poultry industry. Though it is not our primary objective in conducting this study, following the method presented here for assignment of ontogenetic age to ostrich eggshell may permit more extensive study of hatching rates of ostrich in the wild, where dead-in-shell chicks are likely to be consumed by predators or scavengers and cannot be used to perform morphometric assessments. Eggshell, on the other hand may be collected from wild ostrich nests and used to generate estimates of overall hatching rates for wild clutches.

Finally, as described previously for turkey eggs (*G. meleagris*, see Beacham and Durand, 2007), we also noted that ostrich eggshell calcite resorption is impeded by the presence of the air sac. The air sac appears to shield regions of the mammillary layer (Fig. 3 and Supp. Fig. 6), such that the lack of erosion features on a fragment of eggshell of unknown ontogenetic age can present a false positive signal of an early stage of embryonic development. It is thus recommended when possible that samples identifiable to taxon be selected from the equator region based

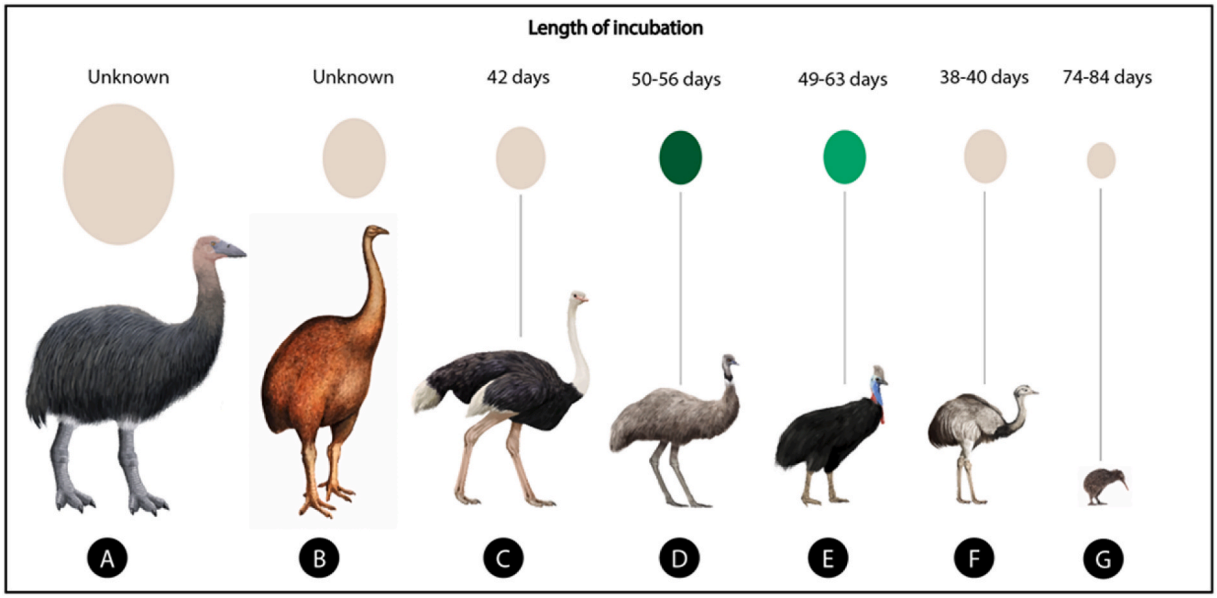

Fig. 11. A subset of ratite species, their eggs (approximately scaled and colored relative to one another), and lengths of egg incubation: A) elephant bird (extinct; Aepyornithidae sp.); B) moa (extinct; Dinornithiformes sp.); C) ostrich (extant; *Struthio* sp.); D) emu (extant; *Dromaius* sp.); E) cassowary (extant; *Casuarius* sp.); F) rhea (extant; *Rhea* sp.); G) kiwi (extant; Apterygidae sp.).

Table 8
Classification matrix for visual identification of ostrich eggshell.

	Correct Classifications – Number and Percentage					
	Early (21)		Middle (14)		Late (7)	
Analyst 1	21	100%	3	21%	3	43%
Analyst 2	13	62%	5	55%	5	71%
Analyst 3	21	100%	3	21%	7	100%

on the documented curvature of eggs belonging to the species in question (see Stoddard et al., 2017).

4. Conclusions

Using ostrich (*Struthio c. australis*) as our model species, our objectives were to 1) quantitatively model changes in eggshell microstructures that are correlated with ontogeny and compare a statistical approach with visual identification, 2) test whether our statistical model successfully predicts the ontogenetic age of eggshell of other avian taxa, and 3) conduct a sensitivity analysis to test the robustness of our model given the issue of archaeological eggshell diagenesis. This work highlights the potential to elucidate patterns of human exploitation of avian

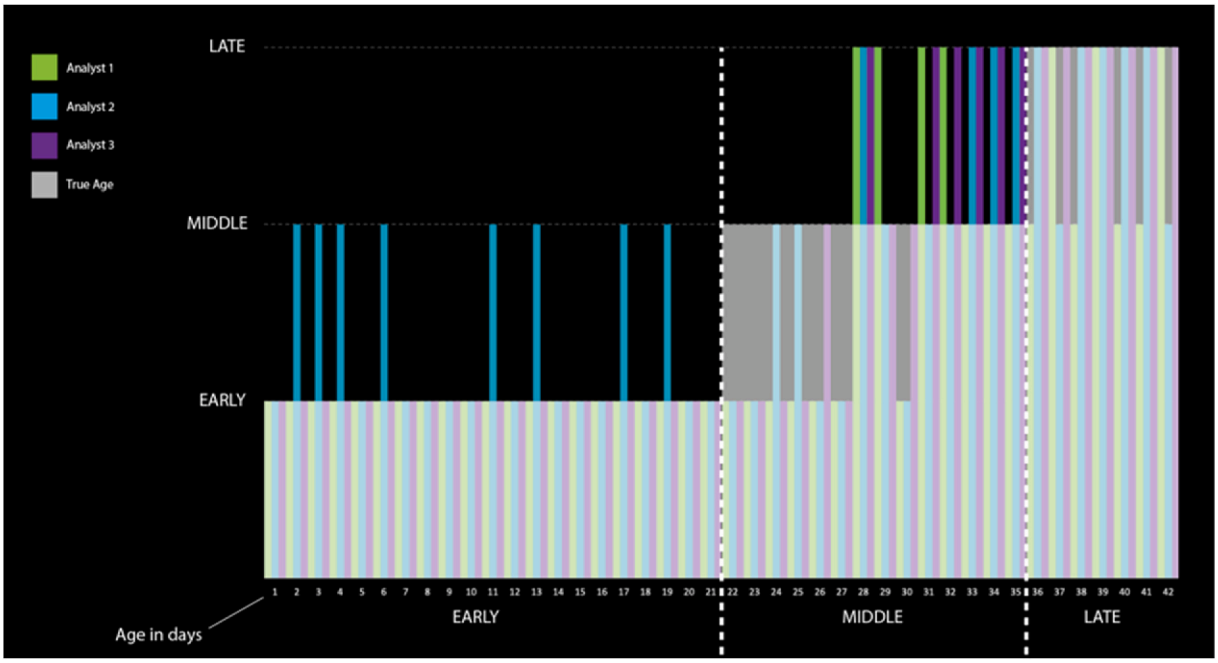

Fig. 12. Visual classification of developmental stage of ostrich eggshell versus true ontogenetic age.

eggs in the archaeological record by identifying eggs that hatched naturally versus eggs that may have been harvested for human consumption. This approach also makes it possible to investigate dietary preferences for eggs at different stages of embryonic development. Eggs identified as having been harvested during late stages of development may be evidence of a preference for consuming developed chick embryos (e.g. balut), as opposed to yolk and albumen (Table 2).

We conclude that our 3-stage statistical model successfully predicts the ontogenetic age of early stage eggs but is less successful at accurately classifying the age of late and especially of middle stage eggs. Middle stage eggs are particularly difficult to classify accurately, regardless of whether we use one or four roughness parameters as our predictor variables. This could suggests that middle stage eggs vary significantly in the rate of eggshell resorption, and perhaps in the rate of embryonic growth. Misclassification of "Middle" stage eggs could also be attributed to the fact that there is potential for them to be mis-classified as "Early" at the beginning of the "Middle" stage, and as "Late" at the end, whereas "Early" and "Late" stage eggs primarily have potential for misclassification either at the beginning or end of the stage. Our 2-stage model was more successful overall at distinguishing "Early" vs. "Late" stage eggs, except during the 4-day period immediately preceding embryo bone ossification.

The erosion of eggshell mammillary cones has been described as a predictable, time-dependent process in turkeys (Beacham and Durand, 2007). However, we observed a significant degree of variability in surface roughness measurements, particularly in the "Middle" stage, making classification of eggshell ontogenetic age difficult (see Supp. Fig. 12). Visual inspection was less reliable than our predictive model, particularly considering the significant intra-analyst variability in classifications of eggshells of all stages. The reliability of visual inspection of archaeological eggshell is also likely to be impeded by diagenesis (see Supp. Fig. 1 for an archaeological example). We thus recommend the adoption of a quantitative modeling approach for the analysis of eggshell ontogenetic age. Our approach provides probabilities of successful classification, including in the case of weathered archaeological eggshell, that are essential for interpreting results.

Though the methods of model setup presented here can be applied to other avian species, our results suggest that species-specific models are likely to be more successful at correctly classifying eggs. We were interested in developing a model that could be used to study eggshell of extinct ratites, including elephant birds (Aepyornithidae) and moa (Dinornithiformes), for which establishing a comparative series of eggshell of known ontogenetic age is impossible. Our results indicate that the methods and models developed here are useful in analyzing assemblages of eggshell from taxa that have similar incubation windows and embryonic growth trajectories to ostrich. Our models are particularly suitable for the analysis of eggshell belonging to other members of the ratite group (Fig. 11). For extinct ratites, such as Madagascar's elephant birds and New Zealand's moas (Fig. 11), the length of the incubation window is unknown. Ostriches, however, remain the largest living ratites and are closer to these extinct giants in terms of their body size and egg-to-body-size ratio than any other extant taxon. Our ostrich models are thus the best available for the analysis of elephant bird and moa eggshell morphology. Applied to archaeological assemblages, the methods we have developed can reveal significant new information regarding human interaction with these extinct birds and the potential contribution of egg harvesting to human economies and avian extinction (Giardina, 2019). Our methods may also have applications to wildlife management, particularly in terms of monitoring the reproductive ecology of vulnerable species by offering an approach to estimating hatching rates or time of mortality in wild clutches.

Finally, despite the challenges of collecting oftentimes small fragments of eggshell, we emphasize the utility of micro-stratigraphic excavation and sifting protocols (hand and trowel and 2 mm mesh) that allow for the recovery of even very small eggshell fragments from the archaeological record (Tellkamp, 2019). Although eggshell diagenesis reduces the likelihood of correctly classifying eggshell according to ontogenetic age, our sensitivity analysis provides probability estimates of the accuracy of classification under different preservation conditions. Future studies of eggshell morphology and other characteristics using the models and data presented here should prove fruitful in enhancing understanding of human-avian interactions around the world.

Declaration of competing interest

The authors declare that there is no conflict of interest.

Acknowledgements

Funding and research permissions.

This work was supported by a Smithsonian National Museum of Natural History Peter Buck Postdoctoral Fellowship (KD) and a National Science Foundation Postdoctoral Fellowship in Biology (#1523857; TF).

Dr. Annie Antonites (the Heritage Foundation, Pretoria, SA) and Dr. Xander Antonites (University of Pretoria) provided input and assisted with the export of *Struthio* eggshell samples from South Africa. Mr. Chris Milensky (Smithsonian, NMNH) assisted with the import of *Struthio* eggshell samples into the United States.

Dr. Tim Rose (Smithsonian, NMNH) assisted with the preparation of Micro-CT samples and provided access to a low-speed diamond saw.

Julie Anderson (Penn State University, Materials Research Institute) assisted with 2D SEM imaging of ratite eggshell samples.

Drs. Given Harper and William Jaeckle (Illinois Wesleyan University) provided samples of modern ratite eggshell of unknown ontogenetic age that were used in experiments with different imaging protocols.

Dr. Jacob Musser (the European Molecular Biology Laboratory) provided emu eggshell samples of known ontogenetic age.

Dr. Emily Durham (Penn State Anthropology) developed the staining protocol for modern eggshell and stained the samples imaged using the Keyence VHX-7000 digital microscope.

Mr. Scott Douglass (Penn State School of Music) provided comments and assistance with data analysis and interpretation.

Use of the Advanced Photon Source, an Office of Science User Facility operated for the U.S. Department of Energy (DOE) Office of Science by Argonne National Laboratory, was supported by the U.S. DOE under Contract No. DE-AC02-06CH11357. Xianghui Xiao and the 2-BM beamline group provided assistance with CT scanning and analysis at the APS facility, Argonne National Lab. Tomography data collections at the Advanced Photon Source beamline 2-BM, Argonne National Laboratory were supported by the U.S. Department of Energy Office of Science (Proposal ID 41887 awarded to Richard Prum). Richard Prum provided access to computing resources for CT reconstructions and data analysis.

Appendix A. Supplementary data

Supplementary data to this article can be found online at https://doi.org/10.1016/j.jas.2021.105442.

Author contributions

KD designed the research with input from all co-authors. ZB collected *Struthio* eggshell samples. KD and SW generated and analyzed 2D and 3D scans using SEM. KD and TF generated and processed micro-CT scans. TT collected and processed OP data. PB and KD developed the statistical model. KD drafted the manuscript and figures with contributions and comments from all authors.

References

Agresti, A., 2013. Categorical Data Analysis. John Wiley & Sons, Hoboken, NJ.

Allentoft, M.E., Heller, R., Oskam, C.L., Lorenzen, E.D., Hale, M.L., Gilbert, M.T.P., Jacomb, C., Holdaway, R.N., Bunce, M., 2014. Extinct New Zealand megafauna were not in decline before human colonization. Proc. Natl. Acad. Sci. Unit. States Am. 111, 4922–4927.
Ar, A., Gefen, E., 1998. Further improving hatchability in artificial incubation of ostrich eggs. In: Huchzermeyer, F.W. (Ed.), International Ratite Congress, pp. 141–147. Oudsthoorn, South Africa.
Assefa, Z., Asrat, A., Hovers, E., Lam, Y., Pearson, O., Pleurdeau, D., 2018. Engraved ostrich eggshell from the middle stone age contexts of goda Buticha, Ethiopia. J. Archaeol. Sci.: Report 17, 723–729.
Beacham, B.E., Durand, S.R., 2007. Eggshell and the archaeological record: new insights into Turkey husbandry in the American southwest. J. Archaeol. Sci. 34, 1610–1621.
Bellairs, R., Osmond, M., 2014. Atlas of Chick Development, third ed. Academic Press, Oxford, UK.
Blom, J., Lilja, C., 2004. A comparative study of growth, skeletal development and eggshell composition in some species of birds. J. Zool. 262, 361–369.
Brand, Z., 2012. Studies on Embryonic Development and Hatchability of Ostrich Eggs. Department of Animal Sciences, University of Stellenbosch.
Brand, Z., Cloete, S.W., Malecki, I.A., Brown, C.R., 2014. Embryonic development in the ostrich (Struthio camelus) during the first 7 days of artificial incubation. Br. Poultry Sci. 55, 68–75.
Brand, Z., Cloete, S.W., Malecki, I.A., Brown, C.R., 2017a. Ostrich (Struthio camelus) embryonic development from 7 to 42 days of incubation. Br. Poultry Sci. 58, 139–143.
Brand, Z., Cloete, S.W., Malecki, I.A., Brown, C.R., 2017b. Dead-in-shell positions of near-term ostrich embryos. S. Afr. J. Anim. Sci. 47, 2–6.
Brooks, A.S., Hare, P.E., Kokis, J.E., Miller, G.H., Ernst, R.D., Wendorf, F., 1990. Dating pleistocene archeological sites by protein diagenesis in ostrich eggshell. Science 248, 60–64.
Burley, R.W., Vadehra, D.V., 1989. The Avian Egg: Chemistry and Biology. John Wiley & Sons, New York, NY.
Buss, A., Keiss, O., 2009. Method for identification of avian species by eggshell microstructure: preliminary study. Acta Universitatis Latviensis 753, 89–98.
Carey, C., 1983. Structure and function of avian eggs. Curr. Ornithol. 1, 69–103.
Chien, Y.C., Hincke, M.T., McKee, M.D., 2009. Ultrastructure of avian eggshell during resorption following egg fertilization. J. Struct. Biol. 168, 527–538.
Clarke, S.J., Miller, G.H., Murray-Wallace, C.V., David, B., Pasveer, J.M., 2007. The geochronological potential of isoleucine epimerisation in cassowary and megapode eggshells from archaeological sites. J. Archaeol. Sci. 34, 1051–1063.
Conard, N.J., Malina, M., Munzel, S.C., 2009. New flutes document the earliest musical tradition in southwestern Germany. Nature 460, 737–740.
Conrad, C., Jones, E.L., Newsome, S.D., Schwartz, D.W., 2016. Bone isotopes, eggshell and Turkey husbandry at arroyo hondo pueblo. J. Archaeol. Sci.: Report 10, 566–574.
Cusack, M., Fraser, A.C., 2002. Eggshell membrane removal for subsequent extraction of intermineral and intramineral proteins. Cryst. Growth Des. 2, 529–532.
Dirrigl, F.J., Brush, T., Morales-Muñiz, A., Bartosiewicz, L., 2020. Prehistoric and historical insights in avian zooarchaeology, taphonomy and ancient bird use. Archaeological and Anthropological Sciences 12, 1–8.
Donaire, M., López-Martínez, N., 2009. Porosity of late paleocene ornitholithus eggshells (tremp Fm, south-central pyrenees, Spain): palaeoclimatic implications. Palaeogeogr. Palaeoclimatol. Palaeoecol. 279, 147–159.
Ecker, M., Botha-Brink, J., Lee-Thorp, J.A., Piuz, A., Horwitz, L.K., 2015. Ostrich eggshell as a source of palaeoenvironmental information in the arid interior of South Africa: a case study from Wonderwerk Cave. In: Runge, J. (Ed.), Changing Climates, Ecosystems and Environments within Arid Southern Africa and Adjoining Regions: Palaeoecology of Africa. Taylor & Francis Group, London, pp. 95–115.
Freundlich, J.C., Kuper, R., Breunig, P., Bertram, H.-g., Institut, G., Koln, U., Germany, W., 1989. Radiocarbon dating of ostrich eggshells. Radiocarbon 31, 1030–1034.
Giardina, M.A., 2019. Economic anatomy of Rheidae and its implication for the archeological record. Archaeological and Anthropological Sciences 11, 6377–6390.
Hawkins, S., O'Connor, S., Louys, J., 2019. Taphonomy of bird (aves) remains at laili cave, timor-leste, and implications for human-bird interactions during the pleistocene. Archaeological and Anthropological Sciences 11, 6325–6337.
Higham, T., 1994. Radiocarbon dating New Zealand prehistory with moa eggshell: some preliminary results. Quat. Sci. Rev. 13, 163–169.
Jacobson, L., 1987. The size variability of ostrich eggshell beads from Central Namibia and its relevance as a stylistic and temporal marker. S. Afr. Archaeol. Bull. 42, 55–58.
Jacomb, C., Holdaway, R.N., Allentoft, M.E., Bunce, M., Oskam, C.L., Walter, R., Brooks, E., 2014. High-precision dating and ancient DNA profiling of moa (Aves: Dinornithiformes) eggshell documents a complex feature at Wairau Bar and refines the chronology of New Zealand settlement by Polynesians. J. Archaeol. Sci. 50, 24–30.
Janz, L., Elston, R.G., Burr, G.S., 2009. Dating North Asian surface assemblages with ostrich eggshell: implications for palaeoecology and extirpation. J. Archaeol. Sci. 36, 1982–1989.
Johnson, B., Fogel, M., Miller, G.H., 1998. Stable isotopes in modern ostrich eggshell: a calibration for paleoenvironmental applications in semi-arid regions of southern Africa. Geochem. Cosmochim. Acta 62, 2451–2461.
Jonuks, T., Oras, E., Best, J., Demarchi, B., Mänd, R., Presslee, S., Vahur, S., 2017. Multi-method analysis of avian eggs as grave goods: revealing symbolism in conversion period Burials at kukruse, NE Estonia. Environ. Archaeol. 23, 109–122.
Kandel, A.W., 2004. Modification of ostrich eggs by carnivores and its bearing on the interpretation of archaeological and paleontological finds. J. Archaeol. Sci. 31, 377–391.
Kandel, A.W., Conard, N.J., 2005. Production sequences of ostrich eggshell beads and settlement dynamics in the Geelbek Dunes of the Western Cape, South Africa. J. Archaeol. Sci. 32, 1711–1721.
Lapham, H.A., Feinman, G.M., Nicholas, L.M., 2016. Turkey husbandry and use in Oaxaca, Mexico: a contextual study of Turkey remains and SEM analysis of eggshell from the Mitla Fortress. J. Archaeol. Sci.: Report 10, 534–546.
Long, A., Hendershott, R.B., Martin, P.S., 1983. Radiocarbon dating of fossil eggshell. Radiocarbon 25, 533–539.
Mikhailov, K.E., 1987. The principal structure of the avian egg-shell: data of SEM studies. Acta Zoologica Cracoviensis 30, 53–70.
Miller, G., Magee, J., Smith, M., Spooner, N., Baynes, A., Lehman, S., Fogel, M., Johnston, H., Williams, D., Clark, P., Florian, C., Holst, R., DeVogel, S., 2016. Human predation contributed to the extinction of the Australian megafaunal bird Genyornis newtoni approximately 47 ka. Nat. Commun. 7, 10496.
Oskam, C.L., Haile, J., McLay, E., Rigby, P., Allentoft, M.E., Olsen, M.E., Bengtsson, C., Miller, G.H., Schwenninger, J.-L., Jacomb, C., Walter, R., Baynes, A., Dortch, J., Parker-Pearson, M., Gilbert, M.T.P., Holdaway, R.N., Willerslev, E., Bunce, M., 2010. Fossil avian eggshell preserves ancient DNA. Proceedings. Biological sciences/The Royal Society 277, 1991–2000.
Oskam, C.L., Allentoft, M.E., Walter, R., Scofield, R.P., Haile, J., Holdaway, R.N., Bunce, M., Jacomb, C., 2012. Ancient DNA analyses of early archaeological sites in New Zealand reveal extreme exploitation of moa (Aves: Dinornithiformes) at all life stages. Quat. Sci. Rev. 52, 41–48.
Serjeantson, D., 2009. Birds. Cambridge University Press, Cambridge.
Sidell, E., 1993. A Methodology for the Identification of Archaeological Eggshell. Museum Applied Science Center for Archaeology (MASCA), Philadelphia, PA.
Stewart, J.R.M., Allen, R.B., Jones, A.K.G., Kendall, T., Penkman, K.E.H., Demarchi, B., O'Connor, T., Collins, M.J., 2013a. Walking on eggshells: a study of egg use in anglo-scandinavian york based on eggshell identification using ZooMS. Int. J. Osteoarchaeol. 24, 247–255.
Stewart, J.R.M., Allen, R.B., Jones, A.K.G.G., Penkman, K.E.H.H., Collins, M.J., 2013b. ZooMS: making eggshell visible in the archaeological record. J. Archaeol. Sci. 40, 1797–1804.
Stoddard, M.C., Yong, E.H., Akkaynak, D., Sheard, C., Tobias, J.A., Mahadevan, L., 2017. Avian egg shape: form, function, and evolution. Science 1249–1254.
Taivalkoski, A., Holt, E., 2016. The effects of cooking on avian eggshell microstructure. J. Archaeol. Sci.: Report 6, 64–70.
Tellkamp, M.P., 2019. A story told from a small-mesh screen: the importance of songbirds and ground doves to the Guangala people at the El Azúcar archeological site in coastal Ecuador. Archaeological and Anthropological Sciences 11, 6411–6421.
Texier, P.-J., Porraz, G., Parkington, J., Rigaud, J.-P., Poggenpoel, C., Miller, C., Tribolo, C., Cartwright, C., Coudenneau, A., Klein, R., Steele, T., Verna, C., 2010. A Howiesons Poort tradition of engraving ostrich eggshell containers dated to 60,000 years ago at Diepkloof Rock Shelter, South Africa. Proc. Natl. Acad. Sci. U.S.A. 107, 6180–6185.
Texier, P.-J., Porraz, G., Parkington, J., Rigaud, J.-P., Poggenpoel, C., Tribolo, C., 2013. The context, form and significance of the MSA engraved ostrich eggshell collection from Diepkloof Rock Shelter, Western Cape, South Africa. J. Archaeol. Sci. 40, 3412–3431.
Vogel, J.C., Visser, E., Fuls, A., 2001. Suitability of ostrich eggshell for radiocarbon dating. Radiocarbon 43, 133–137.
Wei, Y., d'Errico, F., Vanhaeren, M., Peng, F., Chen, F., Gao, X., 2017. A technological and morphological study of Late Paleolithic ostrich eggshell beads from Shuidonggou, North China. J. Archaeol. Sci. 85, 83–104.
Welvaert, M., Rosseel, Y., 2013. On the definition of signal-to-noise ratio and contrast-to-noise ratio for fMRI data. PloS One 8, e77089.
Windes, T.C., 1987. The use of turkeys at Pueblo Alto based on the eggshell and faunal remains. In: Mathien, F.C., Windes, T.C. (Eds.), Investigations at the Pueblo Alto Complex, Chaco Canyon. Part 2. National Park Service, US Department of the Interior, Santa Fe, NM, pp. 679–687.